JOC Article

Diverse Redox-Active Molecules Bearing Identical Thiol-Terminated Tripodal Tethers for Studies of Molecular Information Storage

Lingyun Wei,[†] Kisari Padmaja,[‡] W. Justin Youngblood,[‡] Andrey B. Lysenko,[‡] Jonathan S. Lindsey,*[,‡] and David F. Bocian*[,†]

Department of Chemistry, University of California, Riverside, California 92521-0403, and Department of Chemistry, North Carolina State University, Raleigh, North Carolina 27695-8204

david.bocian@ucr.edu; jlindsey@ncsu.edu

Received July 1, 2003

To examine the effects of molecular structure on charge storage in self-assembled monolayers (SAMs), a family of redox-active molecules has been prepared wherein each molecule bears a tether composed of a tripodal linker with three protected thiol groups for surface attachment. The redox-active molecules include ferrocene, zinc porphyrin, ferrocene-zinc porphyrin, magnesium phthalocyanine, and triple-decker lanthanide sandwich coordination compounds. The tripodal tether is based on a tris[4-(*S*-acetylthiomethyl)phenyl]-derivatized methane. Each redox-active unit is linked to the methane vertex by a 4,4′-diphenylethyne unit. The electrochemical characteristics of each compound were examined in solution and in SAMs on Au. Redox-kinetic measurements were also performed on the SAMs (with the exception of the magnesium phthalocyanine) to probe (1) the rate of electron transfer in the presence of an applied potential and (2) the rate of charge dissipation after the applied potential is disconnected. The electrochemical studies of the SAMs indicate that the tripodal tether provides a more robust anchor to the Au surface than does a tether with a single site of attachment. However, the electron-transfer and charge-dissipation characteristics of the two tethers are generally similar. These results suggest that the tripodal tether offers superior stability characteristics without sacrificing electrochemical performance.

Introduction

The rational design of molecular-based information storage devices that rely on charge accumulation requires an understanding of the electron-transfer dynamics of diverse redox-active groups attached to electroactive surfaces. In studies of self-assembled monolayers (SAMs) of ferrocenes and porphyrins attached to Au via thiol tethers, we found the two types of molecules to have dramatically different electron-transfer characteristics.[1,2] These differences encompassed both the electron-transfer rates measured in the presence of applied potential and the charge-dissipation rates in the absence of applied potential. In particular, the electron-transfer kinetics for the porphyrins were considerably slower (at least 10-fold) than for the ferrocenes. Triple-decker sandwich coordination compounds composed of porphyrins, phthalocyanines, and lanthanide metals were found to exhibit electron-transfer kinetics intermediate between those of ferrocenes and porphyrins.[2,3] On the other hand, ferrocenes and porphyrins attached via identical tethers on Si gave comparable electron-transfer properties.[4] Because the molecules were tethered via a linker bearing only one surface attachment group, the possibility existed that the distinct electron-transfer characteristics stemmed from different orientations with respect to the surface rather than the different composition of the respective redox-active units.

In the preceding paper, we described the synthesis of phosphonic acid terminated tripodal tethers for attaching redox-active groups to oxide surfaces.[5] The motivation for employing tripodal tethers was to enforce a vertical orientation of the redox-active molecules at a fixed distance from the surface. The tripod employed was built around a tetraarylmethane bearing three phosphonic acid groups. The tetrahedral projection of the aryl groups, of which three provide surface attachment, causes the fourth aryl group to project normal to the surface. For studies on Au or Si, thiol tethers are ideal. A number of tripodal tethers bearing sulfur-containing termini (SH,[6−13]

[†] University of California.
[‡] North Carolina State University.

(1) Roth, K. M.; Liu, Z.; Gryko, D. T.; Clausen, C.; Lindsey, J. S.; Bocian, D. F.; Kuhr, W. G. *Molecules as Components of Electronic Devices*; ACS Symposium Series 844; American Chemical Society: Washington, DC, 2003; pp 51−61.
(2) Roth, K. M.; Gryko, D. T.; Clausen, C.; Li, J.; Lindsey, J. S.; Kuhr, W. G.; Bocian, D. F. *J. Phys. Chem. B* **2002**, *106*, 8639−8648.
(3) Gryko, D.; Li, J.; Diers, J. R.; Roth, K. M.; Bocian, D. F.; Kuhr, W. G.; Lindsey, J. S. *J. Mater. Chem.* **2001**, *11*, 1162−1180.
(4) Roth, K. M.; Yasseri, A. A.; Liu, Z.; Dabke, R. B.; Malinovskii, V.; Schweikart, K.-H.; Yu, L.; Tiznado, H.; Zaera, F.; Lindsey, J. S.; Kuhr, W. G.; Bocian, D. F. *J. Am. Chem. Soc.* **2003**, *125*, 505−517.
(5) Loewe, R. S.; Ambroise, A.; Muthukumaran, K.; Padmaja, K.; Lysenko, A. B.; Mathur, G.; Li, Q.; Bocian, D. F.; Misra, V.; Lindsey, J. S. *J. Org. Chem.* **2004**, *69*, 1453−1460.
(6) Whitesell, J. K.; Chang, H. K. *Science* **1993**, *261*, 73−76.
(7) Fox, M. A.; Whitesell, J. K.; McKerrow, A. J. *Langmuir* **1998**, *14*, 816−820.

10.1021/jo0349476 CCC: $27.50
Published on Web 12/11/2003

CHART 1

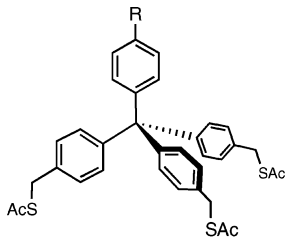

1, R = Br
2, R = I

SAc,[13−15] and SMe[16]) have been described. The tripods incorporate a carbon atom,[6−10,12,13,16] a silicon atom,[14] or an adamantane unit[11,15] at the vertex. A tetraarylmethane-based tripod has been constructed using building block **1** (Chart 1), which bears three *S*-acetylthiomethyl groups and one bromo group.[13] Several redox-active molecules have been attached to the vertical arm of tripod **1**, including oligothiophenes[10,12] and oligothiophene-fullerene dyads.[13]

In this paper, we describe the synthesis of a family of redox-active molecules bearing a tripodal tether with three protected thiol groups. The synthesis makes use of 1,1,1-tris[4-(*S*-acetylthiomethyl)phenyl]-1-(4-X-phenyl)methane, where X = bromo (**1**) or iodo (**2**). The redox-active molecules include a ferrocene, a porphyrin, a phthalocyanine, a ferrocene-porphyrin, and two lanthanide triple decker sandwich coordination compounds (Chart 2). We then describe a series of electrochemical studies designed to evaluate the redox characteristics and the electron-transfer and charge-dissipation rates of the SAMs of the various thiol-derivatized complexes on Au.[17] Taken together, this study provides the foundation for understanding the electron-transfer properties and kinetics of diverse redox-active molecules in a controlled environment on an electroactive surface.

Results and Discussion

1. Synthesis. A. Tripodal Tethers. The *S*-acetylthio-derivatized tripodal molecules **1**[13] and **2** were chosen as the key building blocks for coupling with a variety of redox-active molecules. The iodo-tripod **2** was developed so that the Pd-mediated coupling with an ethyne-substituted redox-active species could employ milder conditions than those for bromo-tripod **1**. In Pd-mediated coupling reactions with porphyrinic substrates, use of an aryl bromide requires elevated temperature whereas the aryl iodide reacts at room temperature.[18]

SCHEME 1

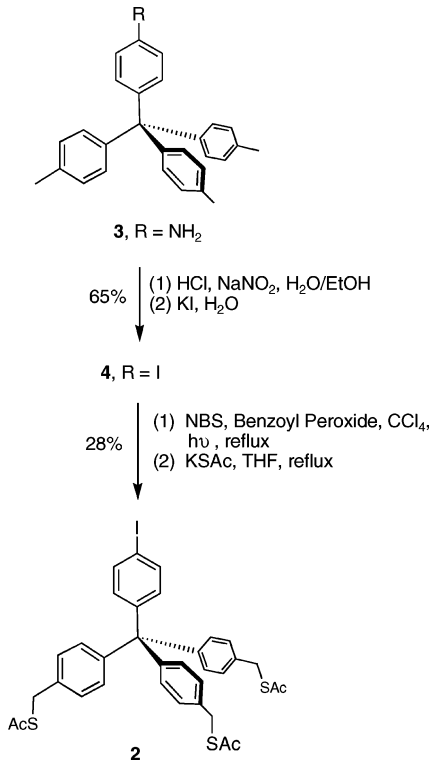

Treating the known compound **3**[19] via a Sandmeyer reaction with aqueous KI provided **4** in 65% yield upon recrystallization. Radical bromination of **4** afforded an inseparable mixture of poorly soluble, brominated products. The mixture was treated with potassium thioacetate, whereupon chromatographic separation proved facile, affording the desired product **2** in 28% yield (Scheme 1).

B. Redox-Active Units. Several redox-active molecules (Chart 3, **5**−**10**) were studied. Compounds **5**,[20] **6**,[21] **7**,[22] **9**,[23] and **10**[24] have been prepared previously. The synthesis of ferrocene-porphyrin **8** is shown in Scheme 2. The mixed condensation of 5-mesityldipyrromethane (**11**),[25] 4-ferrocenylbenzaldehyde (**12**),[26,27] and 4-(3-methyl-3-hydroxybut-1-yn-1-yl)benzaldehyde (**13**)[3] was carried

(8) Fox, M. A.; Li, W.; Wooten, M.; McKerrow, A.; Whitesell, J. K. *Thin Solid Films* **1998**, *327*−*329*, 477−480.
(9) Siiman, O.; Burshteyn, A.; Maples, J. A.; Whitesell, J. K. *Bioconjugate Chem.* **2000**, *11*, 549−556.
(10) Zhu, L.; Tang, H.; Harima, Y.; Yamashita, K.; Hirayama, D.; Aso, Y.; Otsubo, T. *Chem. Commun.* **2001**, 1830−1831.
(11) Kittredge, K. W.; Minton, M. A.; Fox, M. A.; Whitesell, J. K. *Helv. Chim. Acta* **2002**, *85*, 788−798.
(12) Zhu, L.; Tang, H.; Harima, Y.; Yamashita, K.; Aso, Y.; Otsubo, T. *J. Mater. Chem.* **2002**, *12*, 2250−2254.
(13) Hirayama, D.; Takimiya, K.; Aso, Y.; Otsubo, T.; Hasobe, T.; Yamada, H.; Imahori, H.; Fukuzumi, S.; Sakata, Y. *J. Am. Chem. Soc.* **2002**, *124*, 532−533.
(14) Yao, Y.; Tour, J. M. *J. Org. Chem.* **1999**, *64*, 1968−1971.
(15) Li, Q.; Rukavishnikov, A. V.; Petukhov, P. A.; Zaikova, T. O.; Jin, C.; Keana, J. F. W. *J. Org. Chem.* **2003**, *68*, 4862−4869.
(16) Hu, J.; Mattern, D. L. *J. Org. Chem.* **2000**, *65*, 2277−2281.
(17) Note that the terms "thiol tether" and "thiol-derivatized" in the context of SAMs are meant to imply a surface-attached species containing a Au−S bond.
(18) Loewe, R. S.; Lammi, R. K.; Diers, J. R.; Kirmaier, C.; Bocian, D. F.; Holten, D.; Lindsey, J. S. *J. Mater. Chem.* **2002**, *12*, 1530−1552.
(19) Heim, C.; Affeld, A.; Nieger, M.; Vögtle, F. *Helv. Chim. Acta* **1999**, *82*, 746−759.
(20) Ambroise, A.; Wagner, R. W.; Rao, P. D.; Riggs, J. A.; Hascoat, P.; Diers, J. R.; Seth, J.; Lammi, R. K.; Bocian, D. F.; Holten, D.; Lindsey, J. S. *Chem. Mater.* **2001**, *13*, 1023−1034.
(21) Youngblood, W. J.; Gryko, D. T.; Lammi, R. K.; Bocian, D. F.; Holten, D.; Lindsey, J. S. *J. Org. Chem.* **2002**, *67*, 2111−2117.
(22) Yang, S. I.; Li, J.; Cho, H. S.; Kim, D.; Bocian, D. F.; Holten, D.; Lindsey, J. S. *J. Mater. Chem.* **2000**, *10*, 283−296.
(23) Balakumar, A.; Lysenko, A. B.; Carcel, C.; Malinovskii, V. L.; Gryko, D. T.; Schweikart, K.-H.; Loewe, R. S.; Yasseri, A. A.; Liu, Z.; Bocian, D. F.; Lindsey, J. S. *J. Org. Chem.* **2004**, *69*, 1435−1443.
(24) Li, J.; Gryko, D.; Dabke, R. B.; Diers, J. R.; Bocian, D. F.; Kuhr, W. G.; Lindsey, J. S. *J. Org. Chem.* **2000**, *65*, 7379−7390.
(25) (a) Lee, C.-H.; Lindsey, J. S. *Tetrahedron* **1994**, *50*, 11427−11440. (b) Littler, B. J.; Miller, M. A.; Hung, C.-H.; Wagner, R. W.; O'Shea, D. F.; Boyle, P. D.; Lindsey, J. S. *J. Org. Chem.* **1999**, *64*, 1391−1396.
(26) Gryko, D. T.; Zhao, F.; Yasseri, A. A.; Roth, K. M.; Bocian, D. F.; Kuhr, W. G.; Lindsey, J. S. *J. Org. Chem.* **2000**, *65*, 7356−7362.

CHART 2

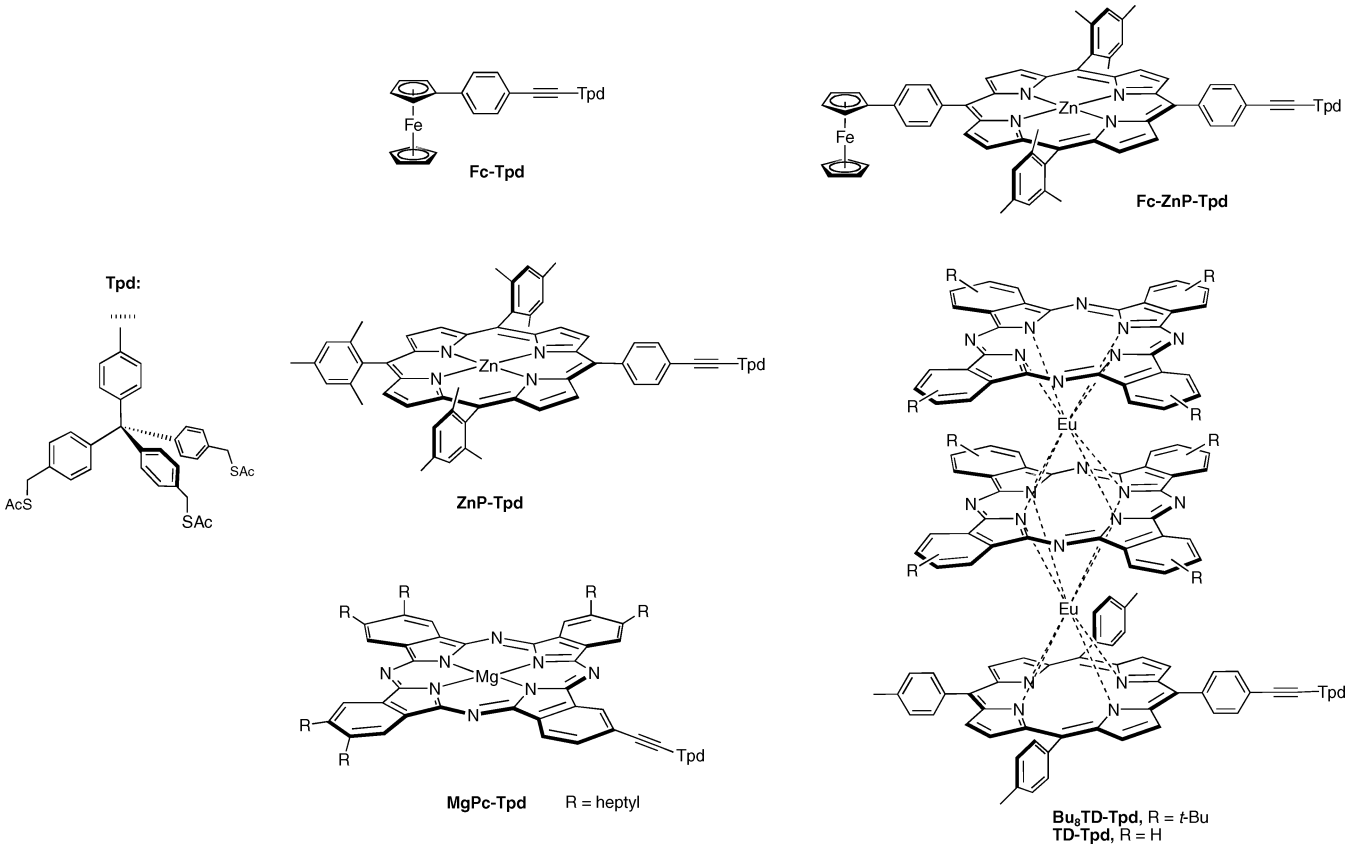

out in CH_2Cl_2 containing 17.8 mM TFA at room temperature. Such catalysis conditions afford reaction without acidolysis of dipyrromethane **11**.[28] The oxidation conditions adopted here were as reported in the literature for the synthesis of ferrocene-porphyrins.[26] Because of the presence of the easily oxidizable ferrocene unit, the acidic reaction mixture was neutralized with DIEA prior to oxidation (because acids are known to increase the oxidation potential of quinones),[29] and the weaker oxidant *p*-chloranil was used instead of DDQ. Chromatographic purification yielded the desired free base porphyrin **14** in 32% yield. Treatment of the latter with zinc acetate gave zinc porphyrin **15** in 40% yield. Reaction of **15** with sodium hydroxide in refluxing toluene proceeded smoothly to give zinc porphyrin **8** in 76% yield.

Several distinct types of triple deckers can be prepared depending on the nature of the three ligands (porphyrin; phthalocyanine) and choice of lanthanide metals.[30] For the studies described herein, we prepared a triple decker of type (Pc)Ln(Pc)Ln(Por), where H_2Pc is a phthalocyanine, H_2Por is a porphyrin; and Ln is a trivalent lanthanide metal ion. The (Pc)Ln(Pc)Ln(Por) triple decker was attractive because rational synthetic methodology[31,32] has recently become available for preparation of such "type c" triple deckers, replacing statistical methods that afford a mixture of different types of triple deckers. For the applications described herein, we employed Eu as the lanthanide.

Ample quantities of triple decker **9** were available from a rational synthesis.[23] The prior synthesis of ethynyl triple decker **10** was achieved via (1) a statistical reaction of porphyrin **16**, $Eu(acac)_3 \cdot nH_2O$, and Li_2Pc that gave trimethylsilylethynyl triple decker **17** in 9.1% yield after extensive chromatography, followed by (2) cleavage of the trimethylsilyl group of **17**.[24] We repeated the synthesis of **10** via a new rational approach to obtain sufficient quantities for the preparation of the tripodal-linked target compound. The rational approach[31,32] entailed treatment of porphyrin **16** with $Eu(acac)_3 \cdot nH_2O$ in 1,2,4-trichlorobenzene (1,2,4-TCB) at reflux (ca. 230−240 °C) to give the porphyrin half-sandwich complex. The formation of the half-sandwich complex is readily observed by a characteristic change of the absorption spectrum.[33] After forming the half-sandwich complex of **16**, $Eu(Pc)_2$ was added. Prolonged heating of $Eu(Pc)_2$ in 1,2,4-TCB at 230−240 °C affords the homoleptic "all-phthalocyanine" triple-decker $[Eu_2(Pc)_3]$, as well as the free base phthalocyanine as a result of fragmentation of the double

(27) (a) Coe, B. J.; Jones, C. J.; McCleverty, J. A.; Bloor, D.; Cross, G. *J. Organomet. Chem.* **1994**, *464*, 225−232. (b) Imrie, C.; Loubser, C.; Engelbrecht, P.; McCleland, C. W. *J. Chem. Soc., Perkin Trans. 1* **1999**, 2513−2523.

(28) Littler, B. J.; Ciringh, Y.; Lindsey, J. S. *J. Org. Chem.* **1999**, *64*, 2864−2872.

(29) Fukuzumi, S.; Ishikawa, K.; Hironaka, K.; Tanaka, T. *J. Chem. Soc., Perkin Trans. 2* **1987**, 751−760.

(30) (a) Weiss, R.; Fischer, J. In *The Porphyrin Handbook*; Kadish, K. M., Smith, K. M., Guilard, R., Eds.; Academic Press: San Diego, CA, 2003; Vol. 16, pp 171−246. (b) Ng, D. K. P.; Jiang, J. *Chem. Soc. Rev.* **1997**, *26*, 433−442.

(31) Chabach, D.; De Cian, A.; Fischer, J.; Weiss, R.; El Malouli Bibout, M. *Angew. Chem., Int. Ed. Engl.* **1996**, *35*, 898−899.

(32) Gross, T.; Chevalier, F.; Lindsey, J. S. *Inorg. Chem.* **2001**, *40*, 4762−4774.

(33) (a) Wong, C.-P.; Venteicher, R. F.; Horrocks, W. D., Jr. *J. Am. Chem. Soc.* **1974**, *96*, 7149−7150. (b) Wong, C.-P. *Inorg. Synth.* **1983**, *22*, 156−162.

CHART 3

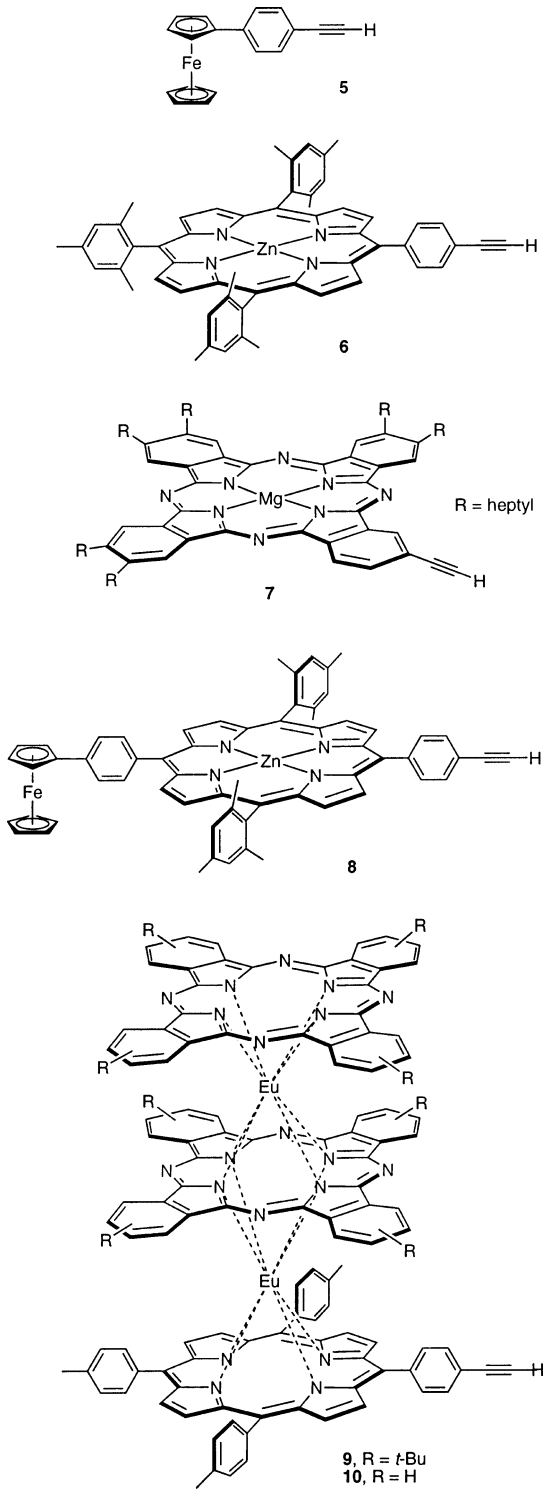

SCHEME 2

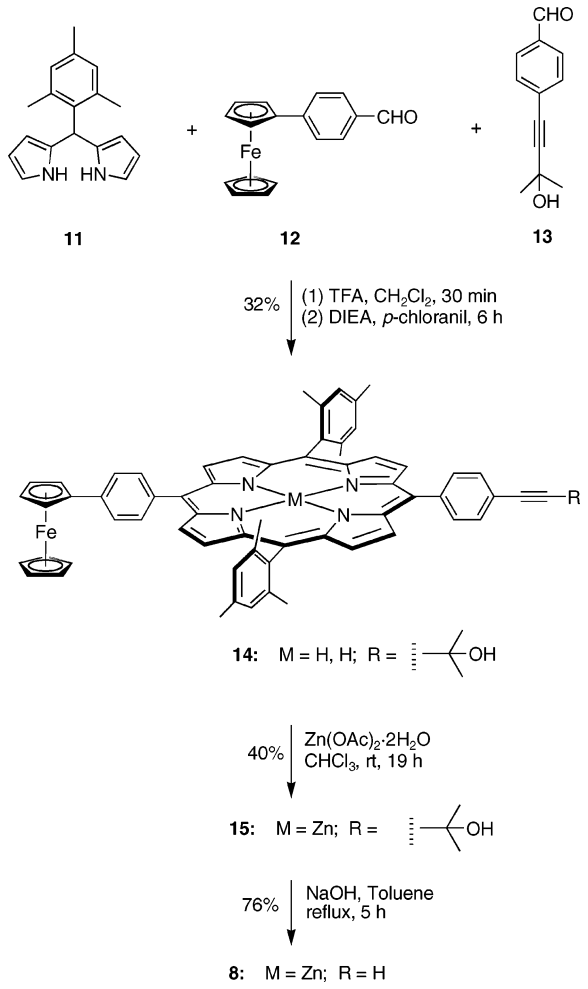

decker $Eu(Pc)_2$. A 33% excess of porphyrin **16** over $Eu(Pc)_2$ was employed in the triple-decker synthesis. The excess **16** in the final reaction mixture was readily recovered by chromatography. This approach afforded triple decker **17** in 34% yield based on the porphyrin starting material (Scheme 3). Treatment with Bu_4NF at room temperature caused cleavage of the TMS group, affording ethynyl triple decker **10** in 89% yield. A distinct advantage of triple decker **10** versus **9** is that the former incorporates unsubstituted phthalocyanines, whereas each phthalocyanine in the latter bears four *tert*-butyl substituents. Each $(t\text{-Bu})_4$-phthalocyanine ligand is composed of a mixture of four regioisomers owing to the position of substitution of the four *tert*-butyl groups at the perimeter of the macrocycle.[34] Accordingly, triple decker **9** is a complex mixture of (inseparable) regioisomers.[3,32] The absence of regioisomers in **10** greatly simplifies the ^{1}H NMR spectrum, facilitating characterization.

C. Tripodal Redox-Active Compounds. The key reaction for the synthesis of the target molecules (Chart 2) is the Pd-mediated Sonogashira coupling of a haloaryl tripod and an ethynylaryl redox-active molecule (Scheme 4). The coupling reactions of **1** and one of each of the ethynyl-substituted redox-active molecules (**5**−**6**, **8**−**10**) were carried out using conditions[18,35] that have been developed for use with porphyrinic substrates [$Pd_2(dba)_3$ and $P(o\text{-tol})_3$ in toluene/TEA at 65 °C]. Such conditions enable reaction in dilute solution (∼2.5 mM) without the use of copper cocatalysts. The coupling reaction of **2** and **7** was carried out similarly, using $Pd_2(dba)_3$ and $AsPh_3$ in toluene/TEA at room temperature. The reactions were

(34) (a) Sommerauer, M.; Rager, C.; Hanack, M. *J. Am. Chem. Soc.* **1996**, *118*, 10085−10093. (b) Pondaven, A.; Cozien, Y.; L'Her, M. *New J. Chem.* **1992**, *16*, 711−718. (c) Pondaven, A.; Cozien, Y.; L'Her, M. *New J. Chem.* **1991**, *15*, 515−516.

(35) Wagner, R. W.; Ciringh, Y.; Clausen, C.; Lindsey, J. S. *Chem. Mater.* **1999**, *11*, 2974−2983.

SCHEME 3

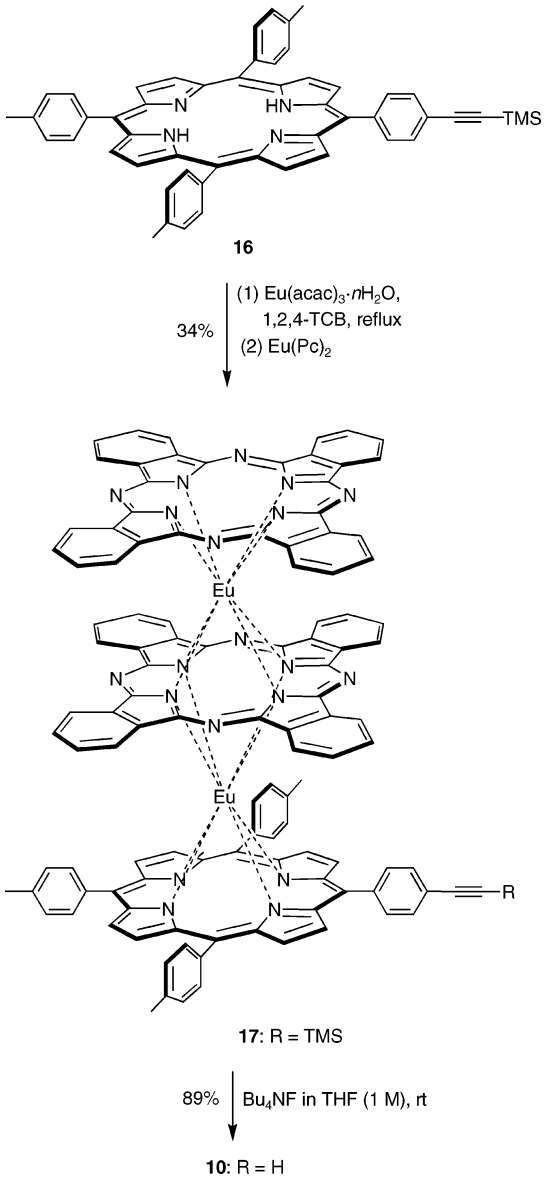

monitored by analytical size-exclusion chromatography (SEC),[36] laser desorption mass spectroscopy (LDMS),[37] and TLC. The target compound from each reaction was purified by column chromatography on silica and, in some cases, preparative SEC. The isolated yields ranged from 14% to 65%. This route provided sufficient quantities for a variety of physical studies.

2. Electrochemical Studies. A. Voltammetric Characteristics of the Complexes in Solution. The solution electrochemical characteristics of the various tripodal complexes were examined prior to the studies of the SAMs of the complexes. The solution voltammetric characteristics of **Fc-Tpd** ($Fc^{0/1+}$ ~0.2 V), **ZnP-Tpd** ($ZnP^{0/1+}$ ~0.6 V; $ZnP^{1+/2+}$ ~0.9 V), **Fc-ZnP-Tpd** ($Fc^{0/1+}$ ~0.2 V; $ZnP^{0/1+}$ ~0.6 V; $ZnP^{1+/2+}$ ~0.9 V), **Bu_8TD-Tpd**

SCHEME 4

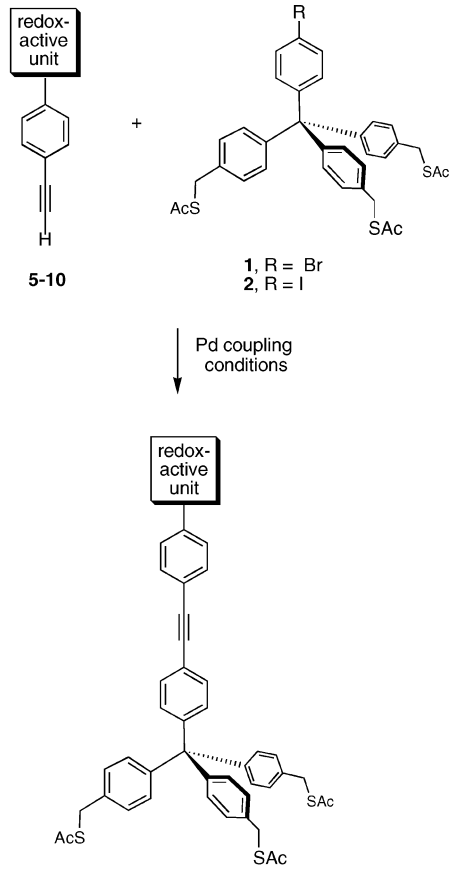

Ethyne	Tripod	Product	Yield (%)
5	**1**	**Fc-Tpd**	31
6	**1**	**ZnP-Tpd**	33
7	**2**	**MgPc-Tpd**	14
8	**1**	**Fc-ZnP-Tpd**	29
9	**1**	**Bu_8TD-Tpd**	65
10	**1**	**TD-Tpd**	18

($TD^{0/1+}$ ~0.1 V; $TD^{1+/2+}$ ~0.6 V; $TD^{2+/3+}$ ~1.0 V; $TD^{3+/4+}$ ~1.3), and **TD-Tpd** ($TD^{0/1+}$ ~0.2 V; $TD^{1+/2+}$ ~0.6 V; $TD^{2+/3+}$ ~1.0 V; $TD^{3+/4+}$ ~1.3 V) (not shown) are essentially identical to those we have previously reported for the complexes with the same redox centers that contain a single *S*-acetylthio group rather than the tripodal *S*-acetylthio tether.[1−3,26,38] This is expected because the linker is relatively long and the *S*-acetylthio group exerts little influence on the redox center.

The solution voltammetry of **MgPc-Tpd** exhibits two oxidative waves (E_1 ~0.15 V; E_2 ~0.90 V) (not shown). Previous studies of magnesium phthalocyanines have typically reported the lower of these two waves, whereas the higher wave has been reported less frequently.[39] The absorption spectrum of the solution of **MgPc-Tpd** exhibited a doublet for the lowest-energy absorption band.

(36) Wagner, R. W.; Johnson, T. E.; Lindsey, J. S. *J. Am. Chem. Soc.* **1996**, *118*, 11166−11180.

(37) (a) Fenyo, D.; Chait, B. T.; Johnson, T. E.; Lindsey, J. S. *J. Porphyrins Phthalocyanines* **1997**, *1*, 93−99. (b) Srinivasan, N.; Haney, C. A.; Lindsey, J. S.; Zhang, W.; Chait, B. T. *J. Porphyrins Phthalocyanines* **1999**, *3*, 283−291.

(38) Gryko, D. T.; Clausen, C.; Roth, K. M.; Dontha, N.; Bocian, D. F.; Kuhr, W. G.; Lindsey, J. S. *J. Org. Chem.* **2000**, *65*, 7345−7355.

Additional electrochemical studies wherein the solution was successively diluted resulted in attenuation of the intensity of both the lower potential voltammetric wave and the higher-energy member of the absorption doublet. However, the lower-potential wave still persisted, even at the lowest concentrations (μM) where the signals were visible. These observations are consistent with the lower-potential voltammetric wave/higher-energy absorption band corresponding to a π-stacked aggregate (perhaps a face-to-face dimer). The fact that the aggregate persists at μM concentrations indicates that the π-stacking interactions are very strong. The pronounced tendency of phthalocyanines to aggregate, even in dilute solution, is well-known.[40] In light of these observations, much of the literature, which reports low potentials for the oxidation of metal phthalocyanines, must be viewed with caution.

B. Voltammetric Characteristics of the Complexes in SAMs. Each *S*-acetyl-protected tripodal complex was examined for formation of a SAM on Au microelectrodes. *S*-Acetylthio groups are known to undergo cleavage upon exposure to gold, resulting in surface attachment (via an S−Au bond) and formation of the SAM without handling free thiols.[41] The procedures and instrumentation for the SAM electrochemical measurements have been described.[42,43]

Representative fast scan cyclic voltammograms (100 V s^{-1}) of the **Fc-Tpd** ($Fc^{0/1+}$ ~0.39 V), **ZnP-Tpd** ($ZnP^{0/1+}$ ~0.71 V; $ZnP^{1+/2+}$ ~1.03 V), **Fc-ZnP-Tpd** ($Fc^{0/1+}$ ~0.38 V; $ZnP^{0/1+}$ ~0.72 V; $ZnP^{1+/2+}$ ~1.05 V), and **TD-Tpd** ($TD^{0/1+}$ ~0.33 V; $TD^{1+/2+}$ ~0.78 V; $TD^{2+/3+}$ ~1.28 V; $TD^{3+/4+}$ ~1.47 V) assemblies are shown in Figure 1. The general voltammetric characteristics of the assemblies are consistent with the formation of relatively homogeneous SAMs wherein the complexes are tethered to Au via the terminal sulfur atoms. The voltammetric characteristics of the **Bu_8TD-Tpd** SAM ($TD^{0/1+}$ ~0.44 V; $TD^{1+/2+}$ ~0.88 V; E $TD^{2+/3+}$ ~1.34 V; $TD^{3+/4+}$ ~1.58) (not shown) are generally similar to those of the **TD-Tpd** SAM; however, the waves are somewhat broader, indicating a less homogeneous assembly. Interestingly, the voltammetry of the **MgPc-Tpd** SAMs exhibits two oxidative waves (E_1 ~0.38 V; E_2 ~1.1 V) (not shown), just as are observed in solution. The intensity of the lower-potential wave is attenuated (relative to the higher potential wave) as the concentration of the complex in the deposition solution is lowered. This observation strongly suggests that both the monomeric and aggregated **MgPc-Tpd** self-assemble on the Au surface. One plausible structure for this aggregate is a face-to-face dimer wherein the tripod of one unit is bound to the Au surface and the tripod of the other points into solution.

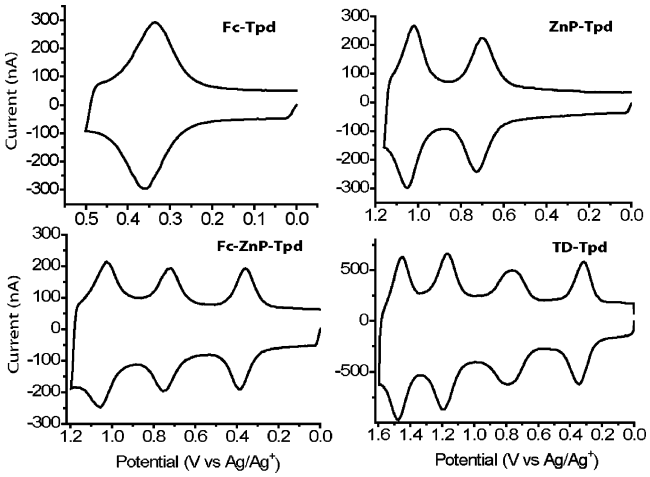

FIGURE 1. Representative fast-scan (100 V s^{-1}) cyclic voltammograms of the **Fc-Tpd** ($\Gamma = \sim 1.6 \times 10^{-11}$ mol cm^{-2}), **ZnP-Tpd** ($\Gamma = \sim 1.1 \times 10^{-11}$ mol cm^{-2}), **Fc-ZnP-Tpd** ($\Gamma = \sim 0.84 \times 10^{-11}$ mol cm^{-2}), and **TD-Tpd** ($\Gamma = \sim 0.86 \times 10^{-11}$ mol cm^{-2}) SAMs. The solvent overlayer was CH_2Cl_2 containing 1.0 M Bu_4NPF_6.

The voltammetric characteristics of the SAMs of the different tripodal ferrocene and porphyrin complexes are generally similar to those we have previously observed for SAMs of complexes with the same redox center and monothiol tethers.[1−3,26,38] As is the case for the SAMs of monothiol-tethered complexes, the formal potential of each of the waves of the tripodal-thiol-tethered complexes in the SAMs is more positive than that observed in solution.[17] The magnitudes of the positive shifts are typically 0.2 V. One clear difference between the voltammetric behavior of the SAMs of the tripodal-thiol- versus monothiol-derivatized complexes is with respect to stability under repeated voltammetric cycling. Under ambient conditions, the tripodal complexes appear to be considerably more stable, as is evidenced by the fact that these assemblies could be subjected to many more (~5-fold) voltammetric cycles before any loss of signal was observed. This observation suggests that all three sulfur atoms in the tripod bind to the Au surface, yielding a generally more robust linkage.

C. Electron-Transfer Characteristics of the SAMs. The standard electron-transfer rate constants (k^0) were measured for each redox state of the **Fc-Tpd**, **ZnP-Tpd**, **Fc-ZnP-Tpd**, and **TD-Tpd** SAMs using swept waveform AC voltammetry (SWAV). These studies were not performed on the **Bu_8TD-Tpd** and **MgPc-Tpd** SAMs. A detailed description of the method, the data analysis procedure, and the relation of k^0 to the measured parameters (the ratio of the peak current to the background current (I_{peak}/I_{bkgd}) as a function of frequency) has been reported elsewhere.[2] Previous studies of other types of porphyrin SAMs have shown that the k^0 values are particularly sensitive to the surface concentration (Γ) when the concentration falls in the range $\Gamma = \sim 1 \times 10^{-12}$ to $\sim 3 \times 10^{-11}$ mol cm^{-2}.[2] In this range, the electron-transfer rates fall by an order of magnitude as the surface concentration increases. Consequently, the surface-

(39) L'Her, M.; Pondaven, A. In *The Porphyrin Handbook*; Kadish, K. M., Smith, K. M., Guilard, R., Eds.; Academic Press: San Diego, CA, 2003; Vol. 16, pp 117−169.
(40) Snow, A. W. In *The Porphyrin Handbook*; Kadish, K. M., Smith, K. M., Guilard, R., Eds.; Academic Press: San Diego, CA, 2003; Vol. 17, pp 129−176.
(41) (a) Tour, J. M.; Jones, L. II; Pearson, D. L.; Lamba, J. J. S.; Burgin, T. P.; Whitesides, G. M.; Allara, D. L.; Parikh, A. N.; Atre, S. V. *J. Am. Chem. Soc.* **1995**, *117*, 9529−9534. (b) Gryko, D. T.; Clausen, C.; Lindsey, J. S. *J. Org. Chem.* **1999**, *64*, 8635−8647.
(42) Schweikart, K.-H.; Malinovskii, V. L.; Yasseri, A. A.; Li, J.; Lysenko, A. B.; Bocian, D. F.; Lindsey, J. S. *Inorg. Chem.* **2003**, *42*, 7431−7446.
(43) Bard, A. J.; Faulkner, L. R. *Electrochemical Methods: Fundamentals and Applications*; Wiley: New York, 2001.

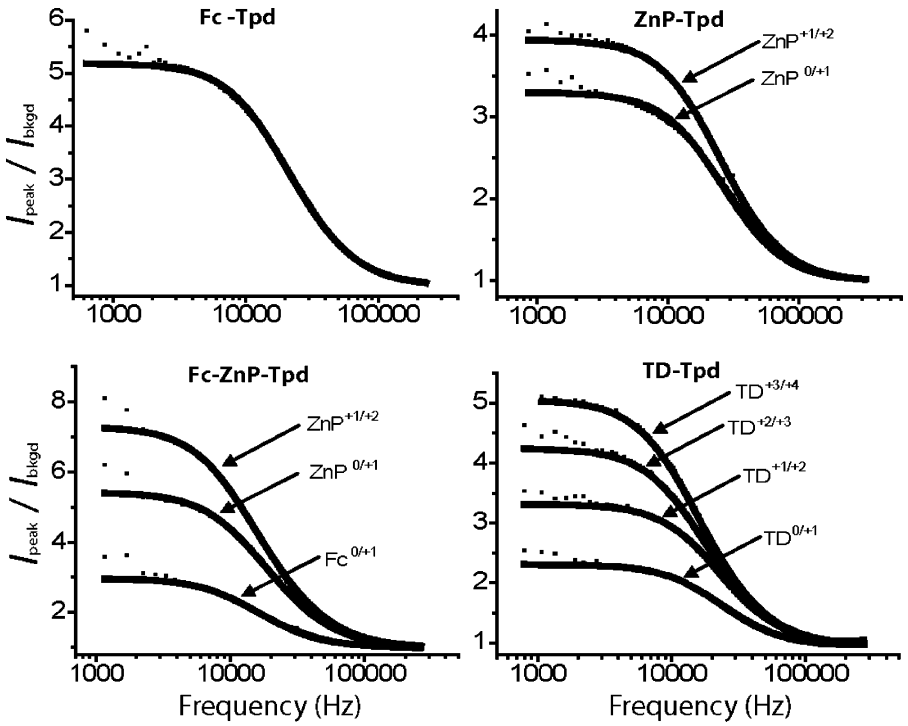

FIGURE 2. I_{peak} /I_{bkgd} (dotted lines) versus frequency for the various cationic states of the **Fc-Tpd**, **ZnP-Tpd**, **Fc-ZnP-Tpd**, and **TD-Tpd** SAMs. The solid lines represent fits to the data using a Randles equivalent circuit. The fitting parameters are as follows: **Fc-Tpd** SAM: $\Gamma = \sim 0.63 \times 10^{-11}$ mol cm^{-2}; $k^0 = \sim 5.0 \times 10^4$ s^{-1}. **ZnP-Tpd** SAM: $\Gamma = \sim 1.5 \times 10^{-11}$ mol cm^{-2}; $ZnP^{0/1+}$, $k_0 = \sim 4.0 \times 10^4$ s^{-1}; $ZnP^{1+/2+}$, $k_0 = \sim 3.1 \times 10^4$ s^{-1}. **Fc-ZnP-Tpd** SAM: $\Gamma = \sim 0.84 \times 10^{-11}$ mol cm^{-2}; $Fc^{0/1+}$, $k^0 = \sim 4.1 \times 10^4$ s^{-1}; $ZnP^{0/1+}$, $k^0 = \sim 4.0 \times 10^4$ s^{-1}; $ZnP^{1+/2+}$, $k^0 = \sim 3.4 \times 10^4$ s^{-1}. **TD-Tpd** SAM: $\Gamma = \sim 0.86 \times 10^{-11}$ mol cm^{-2}; $TD^{0/1+}$, $k^0 = \sim 6.5 \times 10^4$ s^{-1}; $TD^{1+/2+}$, $k^0 = \sim 6.0 \times 10^4$ s^{-1}; $TD^{2+/3+}$, $k^0 = \sim 4.4 \times 10^4$ s^{-1}; $TD^{3+/4+}$, $k^0 = \sim 3.8 \times 10^4$ s^{-1}.

dependence of the standard electron-transfer rates was also investigated.

Representative plots of I_{peak}/I_{bkgd} for the **Fc-Tpd**, **ZnP-Tpd**, **Fc-ZnP-Tpd**, and **TD-Tpd** SAMs are shown in Figure 2. The data for I_{peak} were collected at $E^{n+/(n+1)+}$; the data for I_{bkgd} were collected 0.14 V below $E^{n+/(n+1)+}$. The k^0 values obtained from the fits of the plots of I_{peak}/I_{bkgd} versus frequency at different Γ values are presented in Figures 3 and 4. Inspection of the kinetic data reveals certain general trends: (1) The electron-transfer rates for the SAMs of all the tripodal-thiol-derivatized complexes (with the exception of **Fc-Tpd**, see below) are somewhat slower (~20%) than SAMs of complexes with the same redox center that contain a monothiol tether.[2,3] This result is consistent with the fact that the monothiol-tethered complexes have a phenylethynylphenylmethyl group between the redox center and the sulfur atom, whereas the tripodal-tethered complexes have this group and an additional benzyl group (Chart 1). (2) The electron-transfer rates for all of the oxidation states of all of the SAMs decrease and then level off as the surface coverage increases. (3) The electron-transfer rates for the oxidation states of a particular SAM monotonically decrease with increasing oxidation state. Both of the latter two trends are also consistent with those we have previously reported for SAMs of the analogous monothiol-derivatized complexes.[2,3]

Closer inspection of the kinetics data in Figure 3 reveals certain other trends:

(1) The electron-transfer rates for the **Fc-Tpd** SAM are quite similar to those of the ferrocene unit in the **Fc-ZnP-Tpd** SAM (Figure 3, top). This result indicates that the barrier to electron transfer through the tripodal linker is much higher than the barrier through the zinc porphyrin. Thus, electron transfer through the tripodal linker is rate-limiting. This view is further supported by the observation that the electron-transfer rates for the first oxidation of the zinc porphyrin in the **ZnP-Tpd** SAM are quite similar to those of the ferrocenes in the **Fc-Tpd** and **Fc-ZnP-Tpd** SAMs (cf. Figure 3, top and middle).

(2) The electron-transfer rates for the **Fc-Tpd** SAM are qualitatively similar to those of the first oxidation of the **ZnP-Tpd** SAM. This observation is different from that obtained for the SAMs of the monothiol-derivatized complexes, wherein the electron-transfer rate for the ferrocene was much faster than for the porphyrin.[2] Together, these results strongly suggest that electron-transfer rates for SAMs of the more flexible monothiol-derivatized complexes are influenced by direct interactions of the redox unit with the surface that are precluded in the SAMS of the more rigid (and upright) tripodal-thiol-derivatized complexes. As we have previously discussed, the porphyrin unit in the SAMs of the monothiol-derivatized complexes is prevented from interacting with the surface by the bulky peripheral substituent groups and the tendency of porphyrins to pack in an upright fashion.[4]

(3) The electron-transfer rates for the first and second oxidations of the porphyrin in the **ZnP-Tpd** SAM are generally faster than those of the analogous states for the porphyrin unit in **Fc-ZnP-Tpd** SAM (cf. Figure 3, middle and bottom). This behavior is consistent with the notion that the presence of the oxidized ferrocene unit

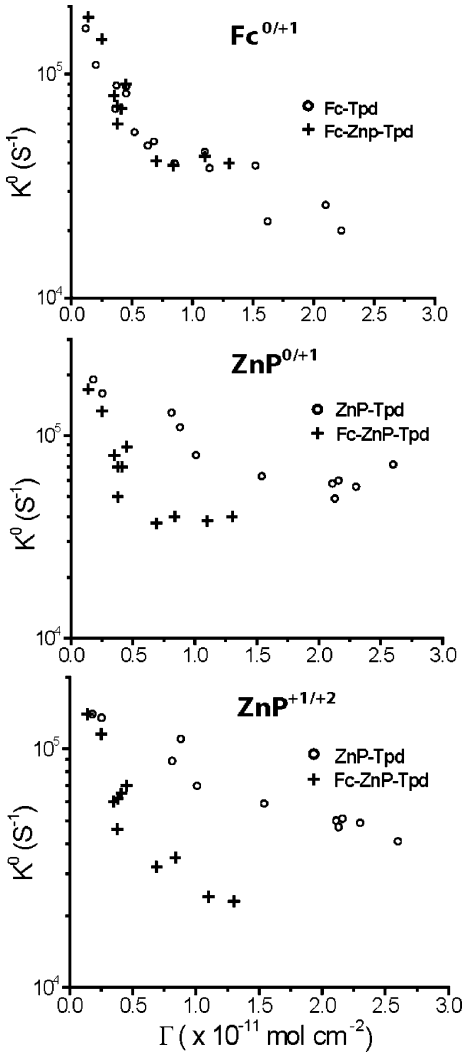

FIGURE 3. Plots of k_0 versus Γ for the various cationic states of the **Fc-Tpd**, **ZnP-Tpd**, and **Fc-ZnP-Tpd** SAMs. The top panel compares the rates for the oxidation of the ferrocene in **Fc-Tpd** and **Fc-ZnP-Tpd**; the middle panel compares the rates for the first oxidation of the porphyrin in **ZnP-Tpd** and **Fc-ZnP-Tpd**; the bottom panel compares the rates for the second oxidation of the porphyrin in **ZnP-Tpd** and **Fc-ZnP-Tpd**.

of the latter complex produces a space-charge that provides a barrier to further oxidation. A similar effect is observed for the **TD-Tpd** SAM for which the rate of each successive oxidation decreases monotonically (Figure 4). However, for the latter SAM, the space-charge effects arise from oxidation of a lower-potential state of a common, delocalized redox center (the π-stack of the complex), whereas in **Fc-ZnP-Tpd**, the effects arise from the oxidation of the lower-potential ferrocene unit that is spatially separated from the zinc porphyrin unit (and distal with respect to the surface).

D. Charge-Retention Characteristics of the SAMs. The charge-retention characteristics of the **Fc-Tpd**, **ZnP-Tpd**, **Fc-ZnP-Tpd**, and **TD-Tpd** SAMs were investigated in parallel with the electron-transfer kinetics. These measurements were made on the same SAMs used for the electron-transfer studies described above. The effect of surface coverage on the charge-retention characteristics was also investigated; however, these studies

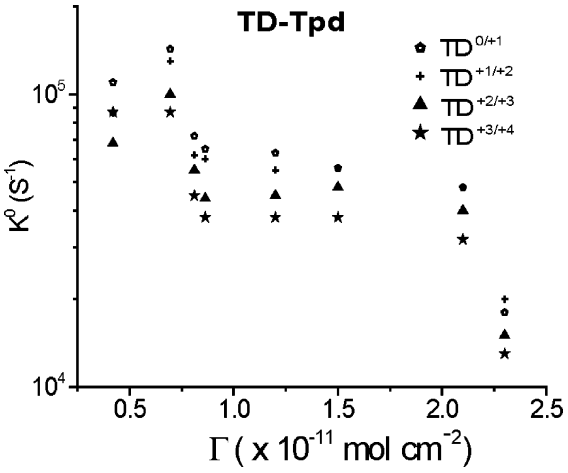

FIGURE 4. Plots of k_0 versus Γ for the four cationic states of the **TD-Tpd** SAMs.

were conducted only at selected coverages in the larger data set for which electron-transfer rates were determined. The charge-dissipation rates were measured using open circuit potential amperometry (OCPA). A detailed description of the method and the data analysis procedure has been reported elsewhere.[44] In previous studies of charge-retention of porphyrin and other triple-decker SAMs, we have found that charge-dissipation rates follow approximately first-order kinetics;[1−3,45] thus, we have characterized these rates in terms of a charge-retention half-life ($t_{1/2}$).

Representative charge-retention data sets are shown for the **Fc-ZnP-Tpd** SAM in Figure 5. The data obtained for the SAMs of the other complexes is similar (not shown). The left panels in the figure show the current-decay transients of the three different oxidized states to the neutral state (Fc^{1+}-ZnP^0-Tpd → Fc^0-ZnP^0-Tpd; Fc^{1+}-ZnP^{1+}-Tpd → Fc^0-ZnP^0-Tpd; Fc^{1+}-ZnP^{2+}-Tpd → Fc^0-ZnP^0-Tpd). The four traces shown for each state are the reductive current measured from the oxidized SAMs after selected disconnect times (10, 20, 30, and 40 s) followed by reconnection at the open circuit potential (wherein molecules that have remained oxidized are reduced). The right panels show the integrated current-decay transients for each time for the three different oxidized states. The integrated current data were fit to a first-order rate law ($r^2 > 0.98$) to determine the $t_{1/2}$ values. The $t_{1/2}$ values at two different surface coverages for the **Fc-Tpd**, **ZnP-Tpd**, **Fc-ZnP-Tpd**, and **TD-Tpd** SAMs are listed in Table 1.

Inspection of the data shown in Table 1 reveals that the charge-retention characteristics of the SAMs generally parallel the electron-transfer characteristics described above. In particular, factors that decrease the value of k^0 also decrease the rate of charge dissipation (i.e., increase $t_{1/2}$). These factors include increasing surface coverage or the presence of charge on the molecule (in the case of the higher oxidation states). All of these trends are consistent with those we have

(44) Roth, K. M.; Lindsey, J. S.; Bocian, D. F.; Kuhr, W. G. *Langmuir* **2002**, *18*, 4030−4040.
(45) Roth, K. M.; Dontha, N.; Dabke, R. B.; Gryko, D. T.; Clausen, C.; Lindsey, J. S.; Bocian, D. F.; Kuhr, W. G. *J. Vac. Sci. Technol. B* **2000**, 18, 2359−2364.

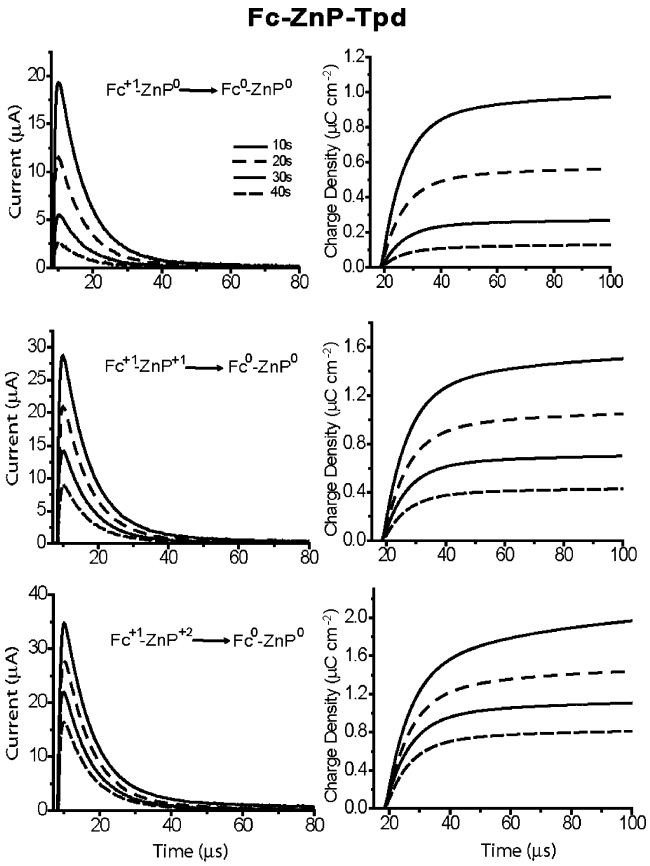

FIGURE 5. Current decay transients (left panels) and integrated current-decay transients (right panels) for the three cationic states of the **Fc-ZnP-Tpd** SAMs.

previously reported for SAMs of the mono-thio-derivatized complexes.[2,3] Certain detailed features of the charge-retention characteristics also parallel the electron-transfer behavior. For example, the $t_{1/2}$ value for the monocation of **Fc-ZnP-Tpd** (ferrocene oxidized) is quite similar to that of the dication (both ferrocene and zinc porphyrin singly oxidized). This result is consistent with the notion that electron flow through the tripodal tether involves a barrier much higher than that for electron transfer from the ferrocene through the zinc porphyrin.

Conclusions

The studies reported herein indicate that the tripodal-thiol tether is an attractive alternative to traditional monothiol tethers. The attractiveness of the tether encompasses both its synthetic and physical characteristics as follows: (1) The preparation of the tether and its attachment to diverse types of redox-active molecules including ferrocenes, porphyrins, and triple-decker sandwich complexes is relatively straightforward. (2) The tripodal-thiol tether provides a more robust anchor to electroactive surfaces such as Au than does the monothiol tether. (3) The redox-kinetic characteristics exhibited by tripodal-thiol-attached molecules are comparable to those of monothiol-attached species. The fact that the tripodal-thiol tethers offer superior stability characteristics without sacrificing electrochemical performance renders these tethers attractive candidates for incorporation in molecular-based information storage media.

TABLE 1. Comparison of Electron-Transfer Rates (k^0) and Charge-Retention Times ($t_{1/2}$) for the SAMs[a]

molecule	Γ ($\times 10^{-11}$ mol cm^{-2})	k^0 ($\times 10^4$ s^{-1})	$t_{1/2}$ (s)
	Fc-Tpd		
	2.7	2.2	22
	0.4	8.0	8
	ZnP-Tpd		
$ZnP^{0/1+}$	0.9	10	17
	2.5	5.5	45
$ZnP^{1+/2+}$	0.9	8	21
	2.5	4.5	53
	Fc-ZnP-Tpd		
$Fc^{0/1+}$	0.45	7.2	12
	0.93	4.1	21
$ZnP^{0/1+}$	0.45	7	14
	0.93	4	25
$ZnP^{1+/2+}$	0.45	6.2	21
	0.93	3.5	30
	TD-Tpd		
$TD^{0/1+}$	0.94	6.5	25
	2.16	2.5	49
$TD^{1+/2+}$	0.94	6	30
	2.16	2.2	53
$TD^{2+/3+}$	0.94	3.4	34
	2.16	1.8	55
$TD^{3+/4+}$	0.94	3.8	45
	2.16	1.5	94

[a] Alterations in the fitting parameters for the SWAV and OCPA data that give equally good fits change the k^0 and $t_{1/2}$ values by ±15%.

Acknowledgment. This work was supported by the DARPA Moletronics Programs (MDA972-01-C-0072) and by ZettaCore, Inc. Mass spectra were obtained at the Mass Spectrometry Laboratory for Biotechnology at North Carolina State University. Partial funding for the facility was obtained from the North Carolina Biotechnology Center and the NSF. We thank Dr. J. R. Diers for assisting with certain of the solution electrochemical measurements.

Supporting Information Available: Complete experimental procedures and relevant spectral data (absorption, mass, and ^{1}H NMR) for all new compounds. This material is available free of charge via the Internet at http://pubs.acs.org.

JO0349476